# A Complete Raman Spectral Assignment of Methanol in C-H Stretching Region.

**ARTICLE** *in* THE JOURNAL OF PHYSICAL CHEMISTRY A · MAY 2013

Impact Factor: 2.69 · DOI: 10.1021/jp400886y · Source: PubMed



**6 AUTHORS**, INCLUDING:

Ke Lin
Xidian University
**21** PUBLICATIONS **192** CITATIONS
SEE PROFILE

Hu Naiyin
University of Science and Technology of China
**6** PUBLICATIONS **31** CITATIONS
SEE PROFILE

Xiaoguo Zhou
University of Science and Technology of China
**51** PUBLICATIONS **316** CITATIONS
SEE PROFILE

Shilin Liu
University of Science and Technology of China
**103** PUBLICATIONS **698** CITATIONS
SEE PROFILE

THE JOURNAL OF PHYSICAL CHEMISTRY A

Article

pubs.acs.org/JPCA

# Complete Raman Spectral Assignment of Methanol in the C−H Stretching Region

Yuanqin Yu,[†,‡] Yuxi Wang,[‡] Ke Lin,[‡] Naiyin Hu,[‡] Xiaoguo Zhou,[‡] and Shilin Liu*[,‡]

[†]School of Physics and Material Science, Anhui University, Hefei, Anhui 230039, China

[‡]Hefei National Laboratory for Physical Sciences at the Microscale, Department of Chemical Physics, University of Science and Technology of China, Hefei, Anhui 230026, China

**ABSTRACT:** In this work, the Raman spectrum of gaseous methanol in the C−H stretching region was investigated by polarized Photoacoustic Raman spectroscopy (PARS). On the basis of the depolarization ratio measurement and density functional theory (DFT) calculations, a complete spectral assignment has been presented. The band at ∼2845 $cm^{-1}$ was assigned to $CH_3$ symmetric stretching, the bands at ∼2925 and ∼2955 $cm^{-1}$ were assigned to two Fermi resonance modes of $CH_3$ bending overtones, and the bands at ∼2961 and ∼3000 $cm^{-1}$ were assigned to out-of-plane and in-plane vibrations of splitting $CH_3$ antisymmetric stretching. Such assignments can clarify the confusions among the previous spectral studies from the different experimental methods and be confirmed by the Raman spectrum of liquid methanol. Furthermore, the large splitting of 39 $cm^{-1}$ between two antisymmetric stretching in gaseous methanol was ascribed to the strong coupling between $CH_3$ and OH groups within methanol molecule because it decreased rapidly in other long-chain alcohol, such as $CH_3CD_2OH$.

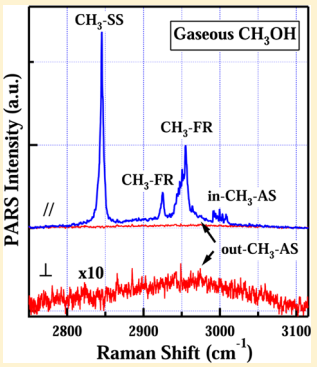


## 1. INTRODUCTION

The C−H functional groups, such as −CH, $-CH_2$, and $-CH_3$, exist widely in organic and biological molecules, and the vibrational spectroscopy in the C−H stretching region from 2700 to 3100 $cm^{-1}$ can be used as a valuable tool to understand molecular conformations, intermolecular interactions, chemical reaction pathways and so on.[1−8] However, it is well-known that the spectra in this region are quite complicated due to the existence of various vibrational modes, including C−H symmetric stretching, antisymmetric stretching, and overtone or combination modes. Furthermore, for $CH_3$ group, the degenerated antisymmetric stretching modes would split into doublets (in-plane and out-of-plane vibrations) when the local symmetry of the $CH_3$ group no longer belongs to $C_{3v}$ point group. Therefore, the spectral assignments in the C−H stretching region tend to be ambiguous, especially for the molecules containing several kinds of C−H groups.

Among all molecules containing C−H groups, methanol ($CH_3OH$) is the simplest but important one used as clean liquid fuels and ideal solvents in industry. Also, methanol is usually taken as an experimental and theoretical benchmark system to investigate large-amplitude torsional motion, the hydrogen bond effect, intramolecular vibrational energy redistribution, and other chemical dynamical processes.[9−17] Many IR, Raman, and SFG spectroscopic studies have been performed to investigate the vibrational spectra of methanol, especially in the C−H stretching region. Generally, one would think that the spectral assignment of methanol in the C−H stretching region has been settled due to its simple structure. In fact, this matter is unsatisfactory up to now because the results from infrared, liquid Raman, and SFG techniques are not consistent and the debates continue.

The experimental data indicate that the vibrational spectra of methanol in the C−H stretching region exhibit two main bands at ∼2834 and ∼2944 $cm^{-1}$ in liquid phase and air/liquid interface. The first band at 2834 $cm^{-1}$ is consistently assigned to the $CH_3$ symmetric stretching. However, for the second band at 2944 $cm^{-1}$, the assignments are in disagreement among the studies by the different experimental methods or even by the same experimental method, as summarized in Table 1. In the infrared spectra, the band at 2944 $cm^{-1}$ in the liquid phase (located at ∼2960 $cm^{-1}$ in gas phase) is assigned to one of the splitting antisymmetric stretching vibrations of $CH_3$ group.[4,18−23] In liquid Raman spectra, some publications assign the band at 2944 $cm^{-1}$ to the $CH_3$ antisymmetric stretching according to the corresponding IR assignments,[11,12,23−25] whereas others assign it to the Fermi resonance of $CH_3$ bending overtone because of its strong polarization.[26−30] In the SFG studies at air/methanol interface, the band at 2944 $cm^{-1}$ is ascribed to the Fermi resonance of bending overtone by various research groups[3,29,31,32] except that one group[33] assigned it to $CH_3$ antisymmetric stretching in the SFG spectrum of methanol on a $TiO_2$ film surface and determined the orientation of methanol on $TiO_2$ on the basis of the intensities of symmetric and antisymmetric stretching. These inconsistent spectral assignments have also been used to interpret relevant dynamical process of methanol. For example, using an ultrafast IR−Raman technique, Dlott et al. investigated the vibration energy redistribution within CH and OH stretching vibrations in liquid methanol or methanol−$CCl_4$

**Received:** January 26, 2013
**Revised:** May 1, 2013
**Published:** May 2, 2013

mixtures and observed the fast energy transfer between the different vibrational modes.[11,12] These explanations on the dynamical process depended on the spectral assignments of methanol in the C−H stretching region.

Recently, using the methods of molecular dynamics (MD) and empirical potential parameter shift analysis (EPSA), Ishiyama et al. qualitatively analyzed the inconsistence on the spectral assignments of liquid methanol in the C−H stretching region.[34,35] To more explicitly clarify the ambiguous spectral assignments, more experimental and theoretical works are needed. In this work, a sensitive nonlinear spectral technique, called polarized photoacoustic Raman spectroscopy (PARS), is used to measure the gas-phase Raman spectrum of methanol. Compared to the infrared, liquid Raman, and SFG methods, the gas-phase Raman spectroscopy exhibits more separated and narrow band shapes and thus has its advantages in investigating the congested C−H stretching region. This is due to the facts that the transition selection rules in Raman are different from those in infrared and gas-phase molecules are free of intermolecular interactions such as hydrogen bonding in the liquid or at the interface. As a result, more spectral details can be observed. Combining these with the depolarization ratio measurements and DFT calculations, we present the complete spectral assignments of gaseous methanol in the C−H stretching region, which can explicitly explain the inconsistencies of the previous studies. In addition, we conduct an experiment on Raman spectra of liquid methanol to confirm the assignments in the gas phase and provided more information on the intermolecular interactions in the liquid phase, especially the hydrogen-bond effect.

## 2. EXPERIMENTAL AND COMPUTATIONAL METHODS

The basic theory and experimental setup of polarized PARS have been fully described in the previous papers,[36−41] but to be complete, a short review is included here. When the frequency difference between two laser beams (pump and Stoke beams) is resonant with a Raman-active vibrational transition, the molecules are transferred to the vibrationally excited state by a stimulated Raman scattering process. Then collisions cause the excitation energy to be converted into local heating. This creates a sound wave that is detected by a microphone. Compared to the direct measurement of weak spontaneous Raman scattering photons, the spectral sensitivity of PARS is greatly increased. On the other hand, using polarized PARS, the Raman depolarization ratio can be accurately determined by measuring and fitting the $I-\theta$ curve because the PARS intensity $I$ is periodically dependent on the cross angle $\theta$ between the polarization directions of two laser beams.[41] More straightforwardly, the intensity ratios of $\theta = 90°$ and $\theta = 0°$ are the depolarization ratio, where $\theta = 90°$ and $\theta = 0°$ mean that the polarization directions of the two laser beams are orthogonal and parallel to each other, respectively. In the present study, the depolarization ratio was obtained by fitting the $I-\theta$ curve because it is more accurate.

In experiment, the second-harmonic output of 532.1 nm from a pulsed Nd:YAG laser (line width 1.0 $cm^{-1}$, pulse width 10 ns) was split into two beams by a quartz wedge. About 90% of the 532.1 nm laser energy directly entered into the dye laser system (line width 0.05 $cm^{-1}$) for generating a tunable Stokes beam (623−638 nm), and the remainder was used as a pump beam for PARS. The two linearly polarized laser beams were focused in the center of the photoacoustic cell with counterpropagating configuration. The photoacoustic signal was detected by a sensitive microphone and monitored by an oscilloscope or averaged by a Boxcar integrator. The energies of pump and Stokes beams were typically 10 and 3 mJ/pulse, respectively, and the sample pressure was kept at 5.0 Torr. The PARS spectrum was normalized to the intensity of the Stokes beam, and the wavelengths of both laser beams were calibrated by a laser wavelength meter with an accuracy of 0.005 nm.

The Raman spectrum of liquid methanol was recorded by a conventional spontaneous Raman technique. The instrument and setup parameters have been described previously.[42,43] Pure methanol was obtained from Aldrich (>99.9%, GC grade) and used as received.

All theoretical calculations, including full geometry optimization and vibrational frequency calculations, were performed using the DFT-B3LYP method with the 6-311++G(d, p) basis set by GAUSSIAN09 software.[44] During calculations, the interactions between the vibrational modes, such as Fermi resonance, were not considered. The calculated frequencies were scaled down by a factor of 0.973 to assist the analysis of experimental spectra.[45]

## 3. RESULTS AND DISCUSSION

**3.1. Gas-Phase Raman Spectra of Methanol in C−H Stretching Region.** The polarized and depolarized Raman spectra of gaseous methanol in the C−H stretching region from 2750 to 3150 $cm^{-1}$ have been recorded with PARS at both parallel ($\theta = 0°$) and perpendicular ($\theta = 90°$) polarization configurations, respectively, as presented in Figure 1a. For visual clarity, the depolarized PARS spectrum is magnified by 10 times and plotted in Figure 1b. As shown in Figure 1a, there is a dramatic change of PARS intensities under two laser polarization configurations. The polarized Raman spectrum shows four prominent bands at 2845, 2925, 2955, and 3000

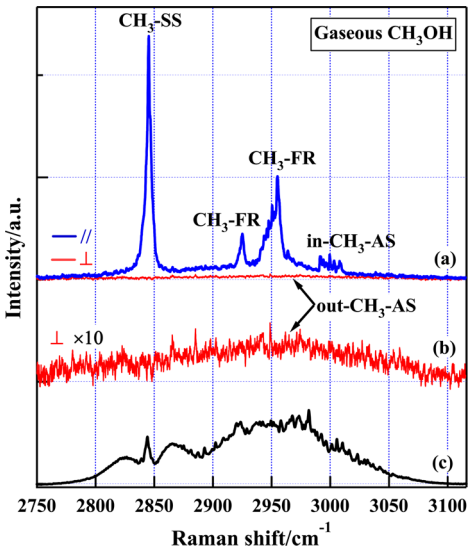


**Figure 1.** (a) Polarized and depolarized PARS spectra of gaseous methanol in the C−H stretching region under parallel (blue line, upper) and perpendicular (red line, lower) laser polarization configurations, respectively. $CH_3$-SS: $CH_3$ symmetric stretching, $CH_3$-FR: $CH_3$ Fermi resonance, in-$CH_3$-AS and out-$CH_3$-AS: in-plane and out-of-plane $CH_3$ antisymmetric stretching. (b) Depolarized PARS spectrum multiplied by a factor of 10 for visual clarity. (c) Infrared spectrum of gaseous methanol in C−H stretching region for comparison.


dx.doi.org/10.1021/jp400886y | J. Phys. Chem. A 2013, 117, 4377−4384

**Table 1. Observed Vibrational Frequencies ($cm^{-1}$) and Raman Depolarization Ratios of Methanol in the Gas and Liquid Phases, as Well as Their Spectral Assignments in the C−H Stretching Region**

| Raman frequency | | | | | | Spectral assignments | | | |
|---|---|---|---|---|---|---|---|---|---|
| $\nu_{gas}$ | $\nu_{liquid}$ | $\Delta\nu$[a] | Inten[b] | $\rho_{gas}$ | $\rho_{liquid}$ | this work | infrared[c] | Raman[liquid] | SFG |
| 2845 | 2834 | 11 | vs | 0.010 | 0.007 | $CH_3$-SS | $CH_3$-SS | $CH_3$-SS | $CH_3$-SS |
| 2925 | 2919 | 6 | m | 0.090 | 0.097 | $CH_3$-FR | | $CH_3$-FR[d] | $CH_3$-FR[f] |
| 2955 | 2944 | 11 | s | 0.038 | 0.007 | $CH_3$-FR | out-$CH_3$-AS | $CH_3$-AS[e] or $CH_3$-FR[d] | $CH_3$-FR[f] or $CH_3$-AS[g] |
| 2961 | 2952 | 9 | vw, br | | | out-$CH_3$-AS | | | |
| 3000 | 2980 | 20 | m | 0.150 | 0.594 | in-$CH_3$-AS | in-$CH_3$-AS | $CH_3$-AS[d] | |

[a] $\Delta\nu$, the frequency difference between the gas and liquid phases. [b] vs, very strong; s, strong; m, medium; vw, very weak; br, broad. [c] Infrared spectral assignment in the gaseous or liquid phases from refs 4 and 18−23. [d] References 27−30. [e] References 11, 12, 24, and 25. [f] References 3, 29, 31, and 32. [g] Reference 33.

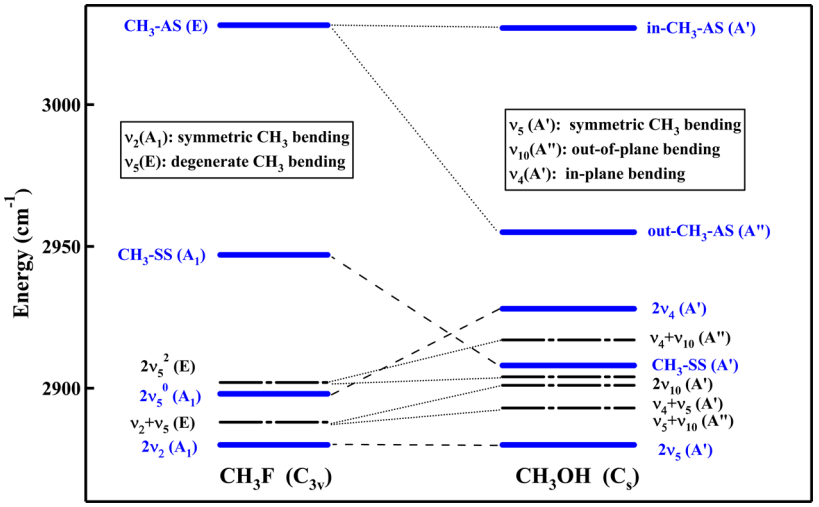


**Figure 2.** Calculated vibrational energy levels of $CH_3OH$ and $CH_3F$ in the C−H stretching region. The molecule of $CH_3F$ was used as an example for $CH_3$ group with rigid $C_{3v}$ symmetry, and the positions of its $2\upsilon_5^0$ and $2\upsilon_5^2$ are schematic for presentation based on the calculated $2\upsilon_5$.

$cm^{-1}$. Among these four bands, the one at 2845 $cm^{-1}$ is the most intense, being 5, 2.5, and 10 times stronger than those at 2925, 2955, and 3000 $cm^{-1}$, respectively. The depolarized spectrum exhibits only one weak and broad band centered at ~2961 $cm^{-1}$, as shown in Figure 1b.

The depolarization ratios have been measured and are summarized in Table 1 as an important means to assist the assignment of the observed spectra. It is known that the depolarization ratio $\rho$ is a symmetry indicator of one Raman-active vibration mode. When using an ideal linearly polarized excitation laser, the $\rho$ value for a symmetric mode is $0 \leq \rho < 0.75$, whereas for an antisymmetric mode $\rho$ equals to 0.75. From Table 1, it can be seen that the values of $\rho$ are very small for the four prominent bands in Figure 1a, indicating that they are strongly polarized and belong to symmetric modes. For the depolarized band at ~2961 $cm^{-1}$ in Figure 1b, the depolarization ratio is not given because it is very weak and overlaps with the high frequency part of intense band at 2955 $cm^{-1}$.

**3.2. Theoretical Calculations on Vibrational Energies of Gaseous Methanol.** To aid the assignment of the experimental spectra, the vibrational energy levels of gaseous methanol in the C−H stretching region have been calculated and are presented in Figure 2.

Usually, the $CH_3$ group is treated as having $C_{3v}$ symmetry in most molecular system,[33,46−48] where the structural parameters such as three C−H bonds are equivalent, and the antisymmetric stretching vibration is doubly degenerated with E symmetry. However, when the $CH_3$ group is attached to OH group to form methanol, the symmetry of $CH_3$ group is lowered to $C_s$ and three C−H bonds are no longer equal. This leads to the splitting of degenerated antisymmetric stretching into two bands. One is the out-of-plane vibration of A″ symmetry (out-$CH_3$-AS); the other is the in-plane vibration of A′ symmetry (in-$CH_3$-AS). To better display the changes of $CH_3$ vibrational energy levels under $C_{3v}$ and $C_s$ symmetry conditions, the vibrational energies of $CH_3F$, which is used as an example with rigid $C_{3v}$ symmetry for the $CH_3$ group, are also calculated in the C−H stretching region and also plotted in Figure 2. It is evident that the antisymmetric stretching is degenerated in $CH_3F$ but splits into two bands in $CH_3OH$ with an interval of 72 $cm^{-1}$. The out-of-plane and in-plane antisymmetric stretching of methanol are described in Figure 3, and the plane refers to H−O−C−H.

Because the Fermi resonance often occurs in the C−H stretching region, the calculated overtones and combinations of $CH_3$ bending modes are also included in Figure 2. The positions of overtones and combinations are double their calculated fundamental. For methanol, the overtones and combinations $2\upsilon_5$, $\upsilon_5 + \upsilon_4$, $2\upsilon_{10}$, and $2\upsilon_4$ are very close to $CH_3$ symmetric stretching fundamental and they have the same A′ symmetry. Therefore, the multiple Fermi resonance can be expected among them. Following the conventional labels, the overtones or combination from Fermi resonance are denoted as $CH_3$-FR, and the symmetric and antisymmetric stretching denoted as $CH_3$-SS and $CH_3$-AS, respectively. It should be


dx.doi.org/10.1021/jp400886y | J. Phys. Chem. A 2013, 117, 4377−4384

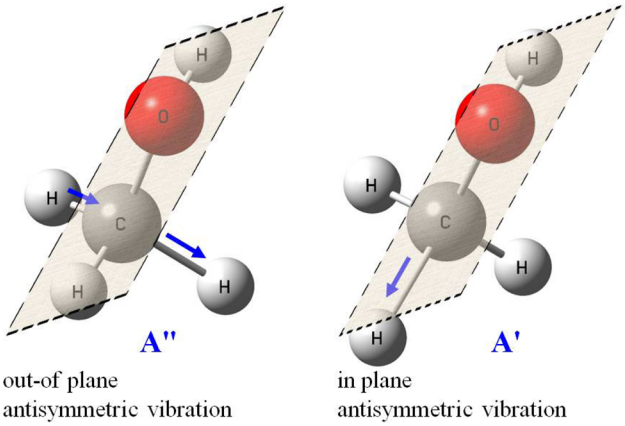


**Figure 3.** Descriptions of out-of-plane and in-plane vibrations of $CH_3$ antisymmetric stretching in methanol. The plane refers to H−O−C−H.

noted that the in-plane $CH_3$-AS of methanol has the same symmetry as the $CH_3$-SS. Thus, the in-plane $CH_3$-AS may also interact with $CH_3$-SS by Fermi resonance, which would lead to the unequal spectral intensity between two splitting bands. This is consistent with the observed PARS spectra of gaseous methanol.

**3.3. Spectral Assignments of Gaseous Methanol in the C−H Stretching Region.** Combined with the measured depolarization ratios and theoretical calculations, the explicit spectral assignments for gaseous methanol in the C−H stretching region are presented in Figure 1 and also listed in Table 1.

According to the theoretical calculations on methanol, the bending overtones and combinations $2\upsilon_5$ (~2880 $cm^{-1}$), $\upsilon_5 + \upsilon_4$ (~2904 $cm^{-1}$), and $2\upsilon_{10}$ (~2906 $cm^{-1}$) are below $CH_3$-SS (~2908 $cm^{-1}$) whereas the overtone $2\upsilon_4$ (~2928 $cm^{-1}$) is above $CH_3$-SS, as indicated in Figure 2. The results from gas-phase infrared spectra of methanol show that the fundamentals of bending modes are located at ~1455 ($\upsilon_5$), ~1477 ($\upsilon_{10}$), and ~1477 $cm^{-1}$ ($\upsilon_4$),[18] which are larger than the corresponding calculated values of ~1440, ~1453, and ~1464 $cm^{-1}$, respectively. Considering the experimental data, we assign the low-frequency intense band at 2845 $cm^{-1}$ as $CH_3$-SS, the high-frequency band at 2925 $cm^{-1}$ as $CH_3$-FR from $2\upsilon_5$ or $\upsilon_5 + \upsilon_4$, and the band at 2955 $cm^{-1}$ as $CH_3$-FR from $2\upsilon_4$ or $2\upsilon_{10}$, as labeled in Figure 1a. For the bands at 2925 and 2955 $cm^{-1}$, we cannot clearly establish which overtone (or combination) principally involves the Fermi resonance because the anharmonicity and Fermi resonance may change the energy positions. The large difference of 63 $cm^{-1}$ (2908 − 2845 = 63) between the calculated and observed $CH_3$-SS can be attributed to the Fermi resonance interaction and the calculation uncertainty. The former factor pushes the unperturbed $CH_3$-SS to shift toward low frequency and the overtones to shift toward high frequency.

Additionally, we attribute the polarized band at 3000 $cm^{-1}$ in Figure 1a to in-plane $CH_3$-AS and the depolarized band centered at 2961 $cm^{-1}$ to out-of-plane $CH_3$-AS according to the corresponding calculated positions at 3027 and 2955 $cm^{-1}$. Such assignment is also consistent with the symmetric properties of A′ for in-plane $CH_3$-AS and A″ for out-of-plane $CH_3$-AS, respectively. The splitting of the above two $CH_3$-AS is not observed in the previous liquid Raman and SFG studies on methanol.[3,11,12,23−32] Here, these two bands are clearly distinguished and assigned in our polarized PARS spectra with the two different polarization configurations.

It can be seen from Figure 1a,b that the out-of-plane $CH_3$-AS at ~2961 $cm^{-1}$ shows a broad band shape and thus overlaps with the $CH_3$-FR at 2955 $cm^{-1}$. This broad feature can be explained by the fact that the antisymmetric band results from $\Delta J = 0, \pm1, \pm2$ rotational transitions whereas the symmetric one mainly from $\Delta J = 0$ transitions (Q branch) in the Raman spectrum. On the other hand, the out-of-plane $CH_3$-AS is very weak and close to the noise level, as shown in Figure 1a. This is in agreement with the general case that the antisymmetric band is weak in Raman measurement whereas strong in infrared. To contrast with the Raman spectrum, we measure the gas-phase infrared spectrum of methanol in the C−H stretching region with FTIR spectrometer (Bruker IFS120HR), as shown in Figure 1c, which is consistent with that in NIST chemistry Web site.[18] It is evident that the band at ~2961 $cm^{-1}$ becomes the most intense in the infrared spectrum, which is very different from the corresponding part in our Raman spectrum. Because of the overlapped spectral features and the opposite behaves of out-of-plane $CH_3$-AS in infrared and Raman cases, the spectral assignments from the different experimental techniques such as infrared, liquid Raman, and SFG are inconsistent, and the detailed interpretations are given in the following.

As mentioned above, the antisymmetric stretching is strong in infrared but weak in Raman. Therefore, in the infrared spectra of methanol, the most intense bands at ~2944 $cm^{-1}$ in the liquid phase and at ~2960 $cm^{-1}$ in the gas phase are assigned to out-of-plane $CH_3$-AS.[4,18−23] Here, the polarized PARS spectrum clearly shows that this band should include the contribution from the $CH_3$ bending overtone. For liquid Raman spectrum of methanol, some literatures assign the band at ~2944 $cm^{-1}$ to $CH_3$-AS according to the corresponding IR assignment,[11,12,23−25] whereas the others assign it to $CH_3$-FR due to its strong polarization,[26−30] as summarized in Table 1. Because of the overlapped spectral features shown in our polarized PARS spectra, both kinds of assignments are incomplete. However, the contribution from out-of-plane $CH_3$-AS is so weak that it can be ignored in the Raman spectrum, as indicated in Figure 1a. Therefore, the band at 2944 $cm^{-1}$ should be contributed by $CH_3$-FR in liquid Raman of methanol. As for the SFG spectrum at the air/methanol interfaces, the explanation for inconsistent assignments is similar to liquid Raman spectrum because the intensity of SFG is the product of infrared dipole transition and Raman tensor elements.

From the above analysis, one can see that our assignments of the Raman spectrum for gaseous methanol can clarify the confusion among the studies from different spectral techniques. Compared to the recent theoretical analysis by molecular dynamics (MD) simulation and empirical potential parameter shift analysis (EPSA) methods,[34,35] the interpretation from the present gas-phase Raman spectra is more explicit and direct.

**3.4. The Splitting of $CH_3$ Antisymmetric Stretching in Different Molecular Systems.** It should be stressed that the direct observation on the splitting between two $CH_3$-AS bands is key to our complete spectral assignments of gaseous methanol. Nevertheless, as mentioned in section 3.2, the antisymmetric stretching is often treated as degeneracy in most molecular systems. MacPhail et al. have systematically investigated the splitting and degeneracy of $CH_3$ antisymmetric stretching in some long-chain alkanes such as *n*-$C_{16}H_{34}$, *n*-$C_{20}H_{40}$, and *n*-$C_{21}H_{44}$.[49,50] Their results indicate that two


dx.doi.org/10.1021/jp400886y | J. Phys. Chem. A 2013, 117, 4377−4384

prominent bands are observed at the extreme low temperature of 9 K with an interval of ~10 $cm^{-1}$ and collapsed into one as the temperature increased. On the basis of their results, the antisymmetric stretching of $CH_3$ group is usually regarded as close degeneracy at room temperature in many molecules.[31,32,51] Here one would ask why methanol has so large a splitting at room temperature.

To answer this question, the Raman spectra of gaseous deuterated ethanol ($CH_3CD_2OH$) in the C−H stretching region are illustrated in Figure 4, which have been reported

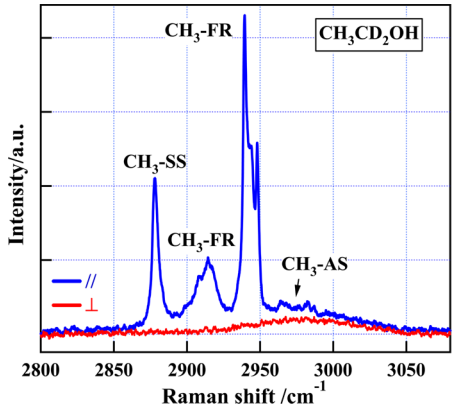


**Figure 4.** Polarized and depolarized PARS spectra of gaseous $CH_3CD_2OH$ in the C−H stretching region measured under parallel (blue line, upper) and perpendicular (black line, lower) laser polarization configurations, respectively.

recently by our group with the same polarized PARS method.[40] The broad feature at 2978 $cm^{-1}$ is assigned to the $CH_3$ antisymmetric stretching of gaseous $CH_3CD_2OH$. However, unlike gaseous methanol, there is no distinguishable splitting between two $CH_3$-AS in $CH_3CD_2OH$, indicating that the splitting of antisymmetric stretching rapidly decreases with the increase of chain length. This conclusion can be interpreted by the following theoretical calculations.

Table 2 lists the calculated out-of-plane and in-plane CH bond lengths and the frequencies of $CH_3$ antisymmetric

**Table 2. Calculated out-of-Plane and in-Plane CH Bond Lengths (Å) and $CH_3$ Antisymmetric Stretching Vibrations ($cm^{-1}$) as Well as Corresponding Depolarization Ratio in Gaseous Methanol and Dueterated Ethanol**

| | $CH_3CD_2OH$[c] | | | $CH_3OH$ | | |
|---|---|---|---|---|---|---|
| molecule | $R_{CH}$[a] | $CH_3$-AS | $\rho$ | $R_{CH}$[a] | $CH_3$-AS | $\rho$ |
| out-of-plane | 1.0919 | 3020 | 0.75 | 1.0970 | 2955 | 0.75 |
| in-plane | 1.0918 | 3028 | 0.722 | 1.0903 | 3027 | 0.511 |
| Δ[b] | 0.0001 | 8 | | 0.0067 | 72 | |

[a] $R_{CH}$, C−H bond length of $CH_3$ group. [b] Δ, differences of out-of-plane and in-plane $CH_3$-AS and CH bonds. [c] Calculations were performed for *trans*-$CH_3CD_2OH$ only, the results for gauch-$CH_3CD_2OH$ are similar and not listed in. The plane of $CH_3CD_2OH$ refers to H−O−C−C−H.

stretching in gaseous $CH_3OH$ and $CH_3CD_2OH$. As indicated by the theoretical calculations, in gaseous $CH_3CD_2OH$, the in-plane CH bond is only 0.0001 Å shorter than the other two out-of-plane CH bond, and the splitting interval between two $CH_3$-AS is 8 $cm^{-1}$. These results are much smaller than the corresponding values of 0.0067 Å and 72 $cm^{-1}$ in gaseous methanol. The more unequal out-of-plane and in-plane CH bonds and the consequent large splitting between two $CH_3$-AS can be ascribed to the strong coupling between $CH_3$ and OH groups within methanol molecule. For $CH_3CH_2OH$ or other long-chain alcohols, the interaction between $CH_3$ and OH groups is weakened due to the existence of $CH_2$ or CH or other groups, and the splitting consequently decreases. This can be further verified by Raman spectra of gaseous deuterated 1-propanol ($CH_3CD_2CD_2OH$) and 2-propanol ($CH_3CDOHCH_3$), and the data will be reported elsewhere. Therefore, in long-chain molecules, where $CH_3$ group is not directly connected to OH group or other strongly electronegative group, two antisymmetric stretching can be deemed as close degeneracy. This conclusion is consistent with the investigations on long-chain alkane systems from MacPhail et al.

Despite close degeneracy of two antisymmetric stretching in gaseous $CH_3CD_2OH$, the out-of-plane and in-plane components can still be distinguished because they behave differently in polarized and depolarized Raman spectra, as shown in Figure 4. For the band at 2978 $cm^{-1}$, several weak polarized peaks are overlapped on the depolarized band. These polarized structures similarly appear in gaseous methanol at ~3000 $cm^{-1}$ and should correspond to the in-plane $CH_3$-AS of gaseous $CH_3CD_2OH$, and the broad and depolarized band at 2978 $cm^{-1}$ corresponds to out-of-plane $CH_3$-AS.

**3.5. Raman Spectra of Liquid Methanol in the C−H Stretching Region.** The polarized and depolarized Raman spectra of liquid methanol in the range from 2750 to 3150 $cm^{-1}$ were measured with the conventional Raman technique and presented in Figure 5.

According to the spectral assignment in gaseous methanol, both polarized and depolarized Raman spectra of liquid methanol are fitted with five component peaks using the Voigt profile,[52−55] and the fitting parameters are listed in Table

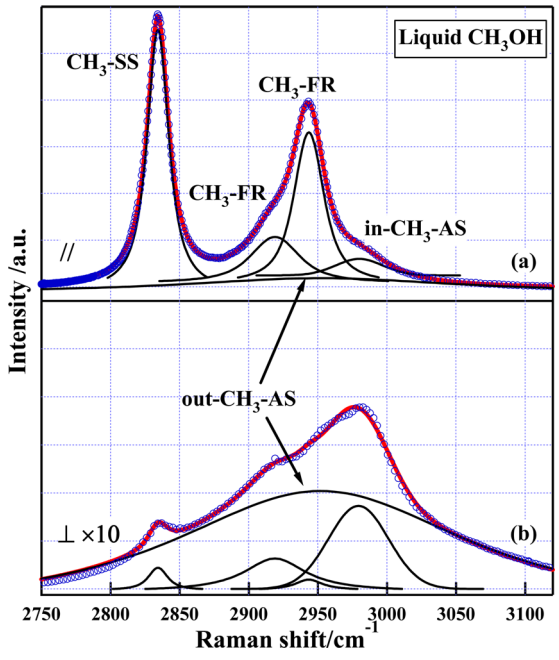


**Figure 5.** Raman spectra of liquid methanol in the C−H stretching region. The solid lines are fittings with the Voigt profiles. (a) Polarized spectrum. (b) Depolarized spectrum magnified by 10 times for visual clarity.


dx.doi.org/10.1021/jp400886y | J. Phys. Chem. A 2013, 117, 4377−4384

Table 3. Fitting Peak Positions ($cm^{-1}$), Areas (au), Gaussian and Lorentzian Width ($cm^{-1}$) of the Polarized and Depolarized Spectra in the C−H Stretching Region of Liquid Methanol Using the Voigt Profile

| | | polarized | | | depolarized | | |
|---|---|---|---|---|---|---|---|
| peak | position | area | Gaussian width | Lorentz width | area | Gaussian width | Lorentz width |
| $CH_3$-SS | 2834 | 1577910 | 6 | 16 | 11285 | 7 | 13 |
| $CH_3$-FR | 2919 | 591398 | 20 | 31 | 57582 | 8 | 25 |
| $CH_3$-FR | 2944 | 1204140 | 12 | 19 | 8089 | 1 | 23 |
| out-$CH_3$-AS | 2952 | 1252020 | 6 | 246 | 941392 | 84 | 220 |
| in-$CH_3$-AS | 2980 | 158270 | 38 | 3 | 94046 | 50 | 1 |

3. The Gaussian, Lorentzian, and Voigt profiles were all tested for the best spectral fit. The Voigt profile was superior to Gaussian and Lorentzian for this liquid spectrum. As shown in Figure 5a,b, the spectral features of liquid methanol are very similar to those in the gas phase except for the band broadening and the changes on the peak positions and intensities. The five bands with the maxima at 2834, 2919, 2944, 2952, and 2980 $cm^{-1}$ correspond to those in the gas phase at 2845, 2925, 2955, 2961, and 3000 $cm^{-1}$ with red shifts of 11, 6, 11, 9, and 20 $cm^{-1}$, respectively. Therefore, the spectral assignments in the gas phase can be applied directly to the liquid phase, as labeled in Figure 5.

From Figure 5a,b, it can be seen that the out-of-plane $CH_3$-AS is very weak in the polarized spectrum of liquid methanol but it becomes relatively apparent in the depolarized spectrum. These behaviors are consistent with those in the gas phase. In previous studies of Raman spectra for liquid methanol, the splitting of $CH_3$ antisymmetric stretching was not considered because the out-of-plane $CH_3$-AS had never been observed.[11,12,23−26,28−30] Another possible reason is that the antisymmetric stretching of $CH_3$ group was often treated as degeneracy in most molecular systems, as explained in section 3.4. Our results indicate that the splitting of antisymmetric stretching still exists in liquid methanol. According to the spectral fit, the interval of two $CH_3$-AS is about 28 $cm^{-1}$ in liquid phase, being 11 $cm^{-1}$ smaller than that in the gas phase. This can be attributed to intermolecular interactions such as the hydrogen-bond interaction, which weakens the coupling between $CH_3$ and OH groups within methanol molecule. A recent study on the microscopic structure of liquid methanol from Raman spectroscopy indicates that liquid methanol comprises combinations of rings or chains of methanol molecules linked with hydrogen bonds and is dominated by structures of trimer, tetramer, and pentamer clusters.[42]

It should be mentioned that unlike the polarized spectrum, there are some deviations between the fitted and observed depolarized spectrum of liquid methanol, as shown in Figure 5b. This may be caused by two factors. First, the Voigt profile cannot completely describe the band shape of Raman spectrum in liquid methanol because methanol is a strong hydrogen-bond system. The usual, accepted theoretical model to interpret the band shape of vibrational peaks perturbed by external interactions such as hydrogen bond is the Kubo model.[56−59] Second, the polarized and depolarized Raman bands of the same vibrational mode appear at different frequency positions.[60,61] In the present spectral fit, the five component peaks in depolarized spectra were fixed at the same positions as those in the polarized one. If the positions of five component peaks in the depolarized spectra are allowed to be different within 7 $cm^{-1}$ from those in the polarized spectra, the depolarized spectrum can also be well fitted. A further investigation on above two factors is being performed for the best spectral fit and will be reported in the future.

## 4. CONCLUSION

In this study, the Raman spectra of gaseous and liquid methanol in the C−H stretching region have been investigated and a complete spectral assignment has been presented with the aid of depolarization ratio measurements and DFT calculations. For the vibrational spectra of methanol, the band at 2944 $cm^{-1}$, which was assigned controversially to $CH_3$-FR or $CH_3$-AS by the different experimental techniques such as infrared, Raman, and SFG spectroscopy, was the overlapping of the $CH_3$-FR and out-of-plane $CH_3$ antisymmetric stretching vibration. Combining with the different behaviors of antisymmetric stretching in infrared and Raman, the confusions in previous spectral studies can be clarified. On the other hand, we explained the large splitting between two antisymmetric stretching vibrations in gaseous methanol by contrast with the Raman spectrum of gaseous $CH_3CD_2OH$ and other long-chain alcohols in the same spectral region, and concluded that the antisymmetric stretching was close degeneracy in the cases that $CH_3$ group is not directly connected to OH group or other strongly electronegative group. These results not only provide reliable groundwork for understanding the structure and dynamical process of methanol in the different environments but also shed new light on the other long-chain molecules containing $CH_3$ group.

## AUTHOR INFORMATION

### Corresponding Author

*E-mail: slliu@ustc.edu.cn.

### Notes

The authors declare no competing financial interest.

## ACKNOWLEDGMENTS

The present work was supported financially by the Natural Science Foundation of China (NSFC, 20903002, 21273211, 91127042) and National Key Basic Research Special Foundation (NKBRSF, 2013CB834602, 2010CB923300) and the 211 Project of Anhui University.

## REFERENCES

(1) Bulkin, B. J.; Krishnan, K. Vibrtional Spectra of Liquid Crystal 0.3. Raman Spectra of Crystal, Cholesteric, and Isotropic Cholesteric Esters, 2800−3100 $cm^{-1}$ Region. *J. Am. Chem. Soc.* **1971**, *93*, 5998−6004.

(2) Silverstein, R. M.; Bassler, G. C.; Morill, T. C. *Spectroscopic Identification of Organic Compound*; John Wiley: New York, 1974.

(3) Guyotsionnest, P.; Hunt, J. H.; Shen, Y. R. Sum-frequency Vibrational Spectroscopy of A Langmuir Film - Study of Molecular-Orientation of a Two-Dimentional System. *Phys. Rev. Lett.* **1987**, *59*, 1597−1600.

(4) Gruenloh, C. J.; Florio, G. M.; Carney, J. R.; Hagemeister, F. C.; Zwier, T. S. C-H Stretch Modes as a Probe of H-bonding in Methanol-Containing Clusters. *J. Phys. Chem. A* **1999**, *103*, 496−502.
(5) Wang, Z.; Pakoulev, A.; Dlott, D. D. Watching Vibrational Energy Transfer in Liquids with Atomic Spatial Resolution. *Science* **2002**, *296*, 2201−3.
(6) Nevin, A.; Osticioli, I.; Anglos, D.; Burnstock, A.; Cather, S.; Castellucci, E. Raman Spectra of Proteinaceous Materials Used in Paintings: A Multivariate Analytical Approach for Classification and Identification. *Anal. Chem.* **2007**, *79*, 6143−6151.
(7) Osticioli, I.; Nevin, A.; Anglos, D.; Burnstock, A.; Cather, S.; Becucci, M.; Fotakis, C.; Castellucci, E. Micro-Raman and Fluorescence Spectroscopy for the Assessment of the Effects of the Exposure to Light on Films of Egg White and Egg Yolk. *J. Raman Spectrosc.* **2008**, *39*, 307−313.
(8) Romero-Pastor, J.; Cardell, C.; Manzano, E.; Yebra-Rodriguez, A.; Navas, N. Assessment of Raman Microscopy Coupled with Principal Component Analysis to Examine Egg Yolk-Pigment Interaction Based on the Protein C-H Stretching Region (3100−2800 $cm^{-1}$). *J. Raman Spectrosc.* **2011**, *42*, 2137−2142.
(9) Laenen, R.; Gale, G. M.; Lascoux, N. IR Spectroscopy of Hydrogen-bonded Methanol: Vibrational and Structural Relaxation on the Femtosecond Time Scale. *J. Phys. Chem. A* **1999**, *103*, 10708−10712.
(10) Chirokolava, A.; Perry, D. S.; Boyarkin, O. V.; Schmid, M.; Rizzo, T. R. Intramolecular Energy Transfer in Highly Vibrationally Excited Methanol. IV. Spectroscopy and Dynamics of ($CH_3OH$)-C-13. *J. Chem. Phys.* **2000**, *113*, 10068−10072.
(11) Iwaki, L. K.; Dlott, D. D. Three-Dimensional Spectroscopy of Vibrational Energy Relaxation in Liquid Methanol. *J. Phys. Chem. A* **2000**, *104*, 9101−9112.
(12) Iwaki, L. K.; Dlott, D. D. Ultrafast Vibrational Energy Redistribution within C-H and O-H Stretching Modes of Liquid Methanol. *Chem. Phys. Lett.* **2000**, *321*, 419−425.
(13) Guo, J. H.; Luo, Y.; Augustsson, A.; Kashtanov, S.; Rubensson, J. E.; Shuh, D. K.; Agren, H.; Nordgren, J. Molecular Structure of Alcohol-Water Mixtures. *Phys. Rev. Lett.* **2003**, *91*, 157401.
(14) Xu, S. C.; Kay, J. J.; Perry, D. S. Doppler-Limited CW Infrared Cavity Ringdown Spectroscopy of the nu(1)+nu(3) OH+CH Stretch Combination Bland of Jet-Cooled Methanol. *J. Mol. Spectrosc.* **2004**, *225*, 162−173.
(15) Kashtanov, S.; Augustson, A.; Rubensson, J. E.; Nordgren, J.; Agren, H.; Guo, J. H.; Luo, Y. Chemical and Electronic Structures of Liquid Methanol from X-ray Emission Spectroscopy and Density Functional Theory. *Phys. Rev. B* **2005**, *71*, 104205.
(16) Rueda, D.; Boyarkin, O. V.; Rizzo, T. R.; Chirokolava, A.; Perry, D. S. Vibrational Overtone Spectroscopy of Jet-Cooled Methanol from 5000 to 14000 $cm^{-1}$. *J. Chem. Phys.* **2005**, *122*, 044314.
(17) Bowman, J. M.; Huang, X.; Handy, N. C.; Carter, S. Vibrational Levels of Methanol Calculated by the Reaction Path Version of Multimode, Using an Ab initio, Full-Dimensional Potential. *J. Phys. Chem. A* **2007**, *111*, 7317−7321.
(18) *NIST Chemistry Webbook* Database at http://webbook.nist.gov.
(19) Falk, M.; Whalley, E. Infrared Spectra of Methanol and Deuterated Methanols in Gas, Liquid, and Solid Phases. *J. Chem. Phys.* **1961**, *34*, 1554−1568.
(20) Bertie, J. E.; Zhang, S. L.; Eysel, H. H.; Baluja, S.; Ahmed, M. K. Infrared Intensities of Liquids-XI - Infrared Refractive-Indexes from 8000 to 2 $cm^{-1}$, Absolute Intergrated-Intensities, and Dipole-Moment Derivatives of Methanol at 25-Degree-C. *Appl. Spectrosc.* **1993**, *47*, 1100−1114.
(21) Bertie, J. E.; Zhang, S. L. L. Infrared Intensities of Liquids XXI: Integrated Absorption Intensities of $CH_3OH$, $CH_3OD$, $CD_3OH$ and $CD_3OD$ and Dipole Moment Derivatives of Methanol. *J. Mol. Struct.* **1997**, *413*, 333−363.
(22) Hu, Y. J.; Fu, H. B.; Bernstein, E. R. Infrared Plus Vacuum Ultraviolet Spectroscopy of Neutral and Ionic Methanol Monomers and Clusters: New Experimental Results. *J. Chem. Phys.* **2006**, *125*, 154306.
(23) Keefe, C. D.; Gillis, E. A. L.; MacDonald, L. Improper Hydrogen-Bonding CH Center Dot Y Interactions in Binary Methanol Systems As Studied by FTIR and Raman Spectroscopy. *J. Phys. Chem. A* **2009**, *113*, 2544−2550.
(24) Atamas, N. A.; Yaremko, A. M.; Bulavin, L. A.; Pogorelov, V. E.; Berski, S.; Latajka, Z.; Ratajczak, H.; Abkowicz-Bienko, A. Anharmonic Interactions and Fermi Resonance in the Vibrational Spectra of Alcohols. *J. Mol. Struct.* **2002**, *605*, 187−198.
(25) Pogorelov, V.; Bulavin, L.; Doroshenko, I.; Fesjun, O.; Veretennikov, O. The Structure of Liquid Alcohols and the Temperature Dependence of Vibrational Bandwidth. *J. Mol. Struct.* **2004**, *708*, 61−65.
(26) Schwartz, M.; Moradiaraghi, A.; Koehler, W. H. Fermi Resonance in Aqueous Methanol. *J. Mol. Struct.* **1980**, *63*, 279−285.
(27) Halonen, L. Theoretical Study of Vibrational Overtone Spectroscopy and Dynamics of Methanol. *J. Chem. Phys.* **1997**, *106*, 7931−7945.
(28) Devendorf, G. S.; Hu, M. H. A.; Ben-Amotz, D. Pressure Dependent Vibrational Fermi Resonance in Liquid $CH_3OH$ and $CH_2Cl_2$. *J. Phys. Chem. A* **1998**, *102*, 10614−10619.
(29) Ma, G.; Allen, H. C. Surface Studies of Aqueous Methanol Solutions by Vibrational Broad Bandwidth Sum Frequency Generation Spectroscopy. *J. Phys. Chem. B* **2003**, *107*, 6343−6349.
(30) Arencibia, A.; Taravillo, M.; Caceres, M.; Nunez, J.; Baonza, V. G. Pressure Tuning of the Fermi Resonance in Liquid Methanol: Implications for the Analysis of High-pressure Vibrational Spectroscopy Experiments. *J. Chem. Phys.* **2005**, *123*, 214502.
(31) Wang, H. F.; Gan, W.; Lu, R.; Rao, Y.; Wu, B. H. Quantitative Spectral and Orientational Analysis in Surface Sum Frequency Generation Vibrational Spectroscopy (SFG-VS). *Int. Rev. Phys. Chem.* **2005**, *24*, 191−256.
(32) Gan, W.; Wu, B.-H.; Zhang, Z.; Guo, Y.; Wang, H.-F. Vibrational Spectra and Molecular Orientation with Experimental Configuration Analysis in Surface Sum Frequency Generation (SFG). *J. Phys. Chem. C* **2007**, *111*, 8716−8725.
(33) Wang, C. Y.; Groenzin, H.; Shultz, M. J. Surface Characterization of Nanoscale TiO2 Film by Sum Frequency Generation Using Methanol as a Molecular Probe. *J. Phys. Chem. B* **2004**, *108*, 265−272.
(34) Ishiyama, T.; Sokolov, V. V.; Morita, A. Molecular Dynamics Simulation of Liquid Methanol. II. Unified Assignment of Infrared, Raman, and Sum Frequency Generation Vibrational Spectra in Methyl C-H Stretching Region. *J. Chem. Phys.* **2011**, *134*, 024510.
(35) Ishiyama, T.; Sokolov, V. V.; Morita, A. Molecular Dynamics Simulation of Liquid Methanol. I. Molecular Modeling Including C-H Vibration and Fermi Resonance. *J. Chem. Phys.* **2011**, *134*, 024509.
(36) Barrett, J. J.; Berry, M. J. Photoacoustic Raman-Spectroscopy (PARS) Using CW Laser Sources. *Appl. Phys. Lett.* **1979**, *34*, 144−146.
(37) Patel, C. K. N.; Tam, A. C. Optoacoustic Raman Gain Spectroscopy of Liquids. *Appl. Phys. Lett.* **1979**, *34*, 760−763.
(38) Yu, Y. Q.; Wang, H.; Shi, Y.; Li, Q. F.; Dai, J. H.; Liu, S. L.; Ma, X. X. Photoacoustic Raman Spectroscopy with Two Counter-prapagating Laser Beams. *Chin. J. Chem. Phys.* **2004**, *17*, 385−389.
(39) Yu, Y. Q.; Zhou, X. G.; Lin, K.; Dai, J. H.; Liu, S. L.; Ma, X. X. Profile Comparison Between the Raman-induced Kerr Effect Spectrum and Photoacoustic Raman Spectrum of Methane. *Acta Phys. Sin.* **2006**, *55*, 2740−2745.
(40) Yu, Y.; Lin, K.; Zhou, X.; Wang, H.; Liu, S.; Ma, X. New C-H Stretching Vibrational Spectral Features in the Raman Spectra of Gaseous and Liquid Ethanol. *J. Phys. Chem. C* **2007**, *111*, 8971−8978.
(41) Yu, Y.; Lin, K.; Zhou, X.; Wang, H.; Liu, S.; Ma, X. Precise Measurement of the Depolarization Ratio from Photoacoustic Raman Spectroscopy. *J. Raman Spectrosc.* **2007**, *38*, 1206−1211.
(42) Lin, K.; Zhou, X.; Luo, Y.; Liu, S. The Microscopic Structure of Liquid Methanol from Raman Spectroscopy. *J. Phys. Chem. B* **2010**, *114*, 3567−3573.
(43) Lin, K.; Hu, N.; Zhou, X.; Liu, S.; Luo, Y. Reorientation Dynamics in Liquid Alcohols from Raman Spectroscopy. *J. Raman Spectrosc.* **2012**, *43*, 82−88.

(44) Frisch, M. J.; Trucks, G. W.; Schlegel, H. B.; Scuseria, G. E.; Robb, M. A.; Cheeseman, J. R.; Scalmani, G.; Barone, V.; Mennucci, B.; Petersson, G. A.; et al. *GAUSSIAN 09*, Reversion B.01; Gaussian, Inc.: Pittsburgh, PA, 2009.
(45) Jarmelo, S.; Maiti, N.; Anderson, V.; Carey, P. R.; Fausto, R. C-alpha-H Bond-stretching Frequency in Alcohols as a Probe of Hydrogen-bonding Strength: A Combined Vibrational Spectroscopic and Theoretical Study of n- 1-D Propanol. *J. Phys. Chem. A* **2005**, *109*, 2069−2077.
(46) Hirose, C.; Yamamoto, H.; Akamatsu, N.; Domen, K. Orientation Analysis by Simulation of Vibrational Sum-Frequency Generation Spectrum - CH Stretching Bands of the Methyl-Group. *J. Phys. Chem.* **1993**, *97*, 10064−10069.
(47) Zhuang, X.; Miranda, P. B.; Kim, D.; Shen, Y. R. Mapping Molecular Orientation and Conformation at Interfaces by Surface Nonlinear Optics. *Phys. Rev. B* **1999**, *59*, 12632−12640.
(48) Wang, J.; Chen, C. Y.; Buck, S. M.; Chen, Z. Molecular Chemical Structure on Poly(methyl methacrylate) (PMMA) Surface Studied by Sum Frequency Generation (SFG) Vibrational Spectroscopy. *J. Phys. Chem. B* **2001**, *105*, 12118−12125.
(49) Macphail, R. A.; Snyder, R. G.; Strauss, H. L. Motional Collapse of Methyle-Group Vibrational Bands. *J. Am. Chem. Soc.* **1980**, *102*, 3976−3976.
(50) Macphail, R. A.; Snyder, R. G.; Strauss, H. L. The Motional Collapse of The Methyle C-H Stretching Vibration Bands. *J. Chem. Phys.* **1982**, *77*, 1118−1137.
(51) Hirose, C.; Akamatsu, N.; Domen, K. Formulas for the Analysis of Surface Sum-Frequency Generation Spectrum by CH Stretching Modes of Methyle and Methylen Groups. *J. Chem. Phys.* **1992**, *96*, 997−1004.
(52) Sundius, T. Computer Fitting of Voigt Profiles to Raman Lines. *J. Raman Spectrosc.* **1973**, *1*, 471−88.
(53) Rothschild, W. G. *Dynamics of Molecular Liquids*; John Wiley and Sons: New York, 1984.
(54) Christian, E. L.; Anderson, V. E.; Harris, M. E. Deconvolution of Raman Spectroscopic Signals for Electrostatic, H-bonding, and Inner-sphere Interactions Between Ions and Dimethyl Phosphate in Solution. *J. Inorg. Biochem.* **2011**, *105*, 538−547.
(55) Painter, P.; Sobkowiak, M.; Park, Y. Vibrational Relaxation in Atactic Polystyrene: A Calculation of the Frequency Correlation Functions of Ring Stretching Modes and Their Variation with Temperature. *Macromolecules* **2007**, *40*, 1738−1745.
(56) D'Amico, F.; Bencivenga, F.; Gessini, A.; Principi, E.; Cucini, R.; Masciovecchio, C. Investigation of Acetic Acid Hydration Shell Formation through Raman Spectra Line-Shape Analysis. *J. Phys. Chem. B* **2012**, *116*, 13219−13227.
(57) Everitt, K. F.; Lawrence, C. P.; Skinner, J. L. Density-Dependent Isotropic Raman Line Shapes in Compressed Room-Temperature Nitrogen. *J. Phys. Chem. B* **2004**, *108*, 10440−10444.
(58) Mariani, L.; Morresi, A.; Cataliotti, R. S.; Giorgini, M. G. Application of the Kubo-Anderson Band Shape Equation to Vibrational Relaxation Studies in the Frequency Domain and to An Improved Determination of Spectral Second Moments from Experimental Data. *J. Chem. Phys.* **1996**, *104*, 914−922.
(59) Morresi, A.; Sassi, P.; Ombelli, M.; Cataliotti, R. S.; Paliani, G. Vibrational Dynamics in Liquid Acetonitrile. Temperature and Concentration Effects in the Non-Ideal $CH_3CN$-$CCl_4$ Mixture. *J. Raman Spectrosc.* **2000**, *31*, 577−585.
(60) Devi, T. G. Study of Vibrational Relaxation and Molecular Reorientation in Liquids: A Raman Spectroscopic Study. *J. Raman Spectrosc.* **2010**, *41*, 1261−1265.
(61) Torii, H.; Giorgini, M. G.; Musso, M. Merged- and Separate-Band Behavior of the C═O Stretching Band in N,N-Dimethylformamide Isotopic Liquid Mixtures: DMF/DMF-d(1), DMF/DMF-d(6), and DMF/DMF-C-13═O. *J. Phys. Chem. B* **2012**, *116*, 353−366.